An Improved Regression Partial Least Squares Method for Quality-Related Process Monitoring of Industrial Control Systems

Zhiqiang Zhang[1], Wenxiao Gao[2], Danlu Yu[3], and Aihua Zhang[1(✉)]

[1] College of Physical Science and Technology, Bohai University, Jinzhou 121013, Liaoning, China
jsxinxi_zah@163.com
[2] Dalian Maritime University, Dalian 116026, Liaoning, China
[3] College of Control Science and Engineering, Bohai University, Jinzhou 121013, Liaoning, China

Abstract. Partial least squares (PLS) is a widely used and effective method in the field of fault detection. However, due to the fact that the standard PLS decomposes the process variable space into two subspaces which are not completely orthogonal, it is insufficient in quality-related fault detection. To solve this problem, principal component regression (PCR) is used to decompose the quality variables of PLS model and realize the reconstruction of the process variable space. In this way, the process variable space is decomposed into highly correlated and highly irrelevant parts of quality variables, and the two are monitored by designing statistics respectively. Furthermore, an adaptive threshold based on the idea of exponential weighted moving average (EWMA) is introduced to reduce the false positives and missed positives caused by the traditional fixed threshold, and this method is named as improved regression partial least squares (RPLS). Finally, linear and nonlinear numerical examples and Tennessee Eastman (TE) processes are used to verify the effectiveness of the proposed method which named improved regression partial least squares (IRPLS). Finally, linear and nonlinear numerical cases and Tennessee Eastman (TE) processes are used to verify the effectiveness of IRPLS. The results show that the proposed method can effectively improve the fault detection rate and algorithm follow-through performance, and reduce false positives.

Keywords: PLS · PCR · EWMA · IRPLS · TE

1 Introduction

With the integration and complexity of modern industrial system, security problems become more and more important. The fault detection method based on analytical model has made outstanding contributions to ensure the normal operation of the system and the safety of people's life and property in the past decades. At the same time, modern

H. R. Karimi and N. Wang (Eds.): S-Cube 2022, LNICST 487, pp. 81–106, 2023.
https://doi.org/10.1007/978-3-031-34899-0_6

industrial system is equipped with a large number of sensors, the collection of data and work log is more convenient and efficient. Data driven fault detection technology [1–5] can excavate and utilize the characteristics of these data to analyze and monitor the running state of the system, has received extensive attention. On the other hand, identifying whether process faults are related to product quality can improve product quality and extend the operating life of equipment by reducing unnecessary downtime and maintenance. PLS [6, 7] is a typical representative of multivariate statistical analysis, which is easy to operate and can efficiently process massive industrial data. It is a widely spread data-driven quality related fault detection technology.

The PLS seeks the maximum correlation between process variables and quality variables by sorting the maximum covariance between input and output matrices, and decompose the process variable space into subspaces related to quality and unrelated to quality, so as to achieve the monitoring purpose of quality-related faults. This also leads to the existence of quality-unrelated parts in the quality-related principal component space (PCS), which affects the accuracy of detection. At the same time, it is possible to leave the mass related part in the residual space (CS), which has a large variance and cannot be detected by SPE statistics [8]. According to the results, what PLS provides is not fully applicable to the actual industrial system. In order to solve such problems, Zhou et al. [9] proposed a post-processing method based on PLS for the first time. This method named total projection to latent structures (TPLS) further decomposes PCS and CS into four Spaces, which more clearly describes the relationship between each space and quality. By further orthogonal decomposition of coefficient matrices between input and output, Yin et al. [10] decompose the process variable space into quality-related and quality- unrelated parts, which are named MPLS. It has been verified that the strategy of this method is simpler and equally effective. Peng [11] and Zhang et al. [12] extend the previous work to apply to nonlinear systems. This kind of method develops rapidly in theory [13] and has been applied in many practical projects [14].

Although these methods have made outstanding contributions to the field of fault detection, there are still many problems worth studying. For example, the ability of some algorithms [15] to detect small faults needs to be improved. In addition, data-driven fault detection techniques often set thresholds [16] based on the method of fixed control limits. To some extent, this method of balancing the relationship between false alarm rate and missed alarm rate will also result in some false alarm and missed alarm. In this paper, a new quality-related fault detection method is proposed to improve the defects of the standard PLS method proposed in the previous paper. The quality variables are decomposed by PCR [17] technology and the relationship between the score matrix and the input matrix is established. By this means, the process variable space is reconstructed to monitor the quality-related and quality-unrelated parts respectively. Furthermore, an idea based on EWMA [18, 19] is introduced to set adaptive threshold, which can ensure the accuracy and integrity of the model by reducing the influence of noise damage data. In this way, the dynamic value with a certain range can be obtained to balance the deviation in the operation of the system more reasonably, which helps to make meaningful decisions. Finally, classical cases are used to verify the effectiveness of the proposed algorithm. The experimental results indicate that the proposed algorithm outperforms the compared algorithms in several aspects such as fault detection rate

(FDR), fault alarm rate (FAR), accuracy for minor faults and tracking performance for specific faults. In summary, the main contributions are outlined as follows.

1) A new spatial decomposition method is proposed, which theoretically solves the problem of incomplete feature space decomposition of the traditional PLS.
2) In order to circumvent the influence of previous samples, this paper introduces more flexible adaptive thresholds in both feature subspaces, which enhances the algorithm's ability to detect some specific faults and is more in line with practical engineering situations.
3) Experiments have been carried out in linear and non-linear numerical cases as well as in the classical TE process and the results show the superior detection results and the high potential of the proposed method for engineering applications.

The structure of this paper is as follows. The Sect. 2 introduces the related work and its disadvantages; The Sect. 3 gives the detailed content of the proposed algorithm. In the Sect. 4, two numerical cases and TE processes are introduced to verify the effectiveness of the algorithm. Finally, in Sect. 5, the work of this paper is summarized and prospected.

2 The Preparatory Work

A. Traditional Partial Least Squares (PLS)
Data are collected through the actual industrial system to form the input data set $U \in R^{N\times m}$ and output data set $Y \in R^{N\times s}$, where N, m and s respectively represent the number of samples, process variables and quality.

By using NIPLS, (U, Y) can be projected into a low-dimensional latent variable space $T = [t_1, t_2, ..., t_A]$, A represents the number of latent variables, usually obtained by cross-validation, etc. After standardization and normalization, U and Y can be decomposed into the following forms by PLS:

$$\begin{aligned} U &= TP^T + E = \hat{U} + \tilde{U} \\ Y &= TQ^T + F = \hat{Y} + \tilde{Y} \end{aligned} \tag{1}$$

where T is called the score matrix, $P \in R^{\mathrm{m}\times A}$ and $Q \in R^{\mathrm{s}\times \mathrm{A}}$ denote the load matrix of U and Y respectively, E and F represent the residuals of U and Y, respectively.

In this model, there is the following relationship:

$$PR^T = R^T P = I_{A\times A} \tag{2}$$

$$T = UR \tag{3}$$

Then the relationship between U and Y can be revealed by the coefficient matrix Δ:

$$Y = TQ^T = URQ^T = U\Delta \tag{4}$$

PLS decomposes a new online sample u into the following

$$u = \hat{u} + e \tag{5}$$

$$\hat{u} = PR^T u \tag{6}$$

$$e = (I - PR^T)u \tag{7}$$

$$t_{ns} = R^T u \tag{8}$$

where t_{ns} represents the score vector for the new sample.

T^2, *SPE* statistics and their corresponding thresholds are widely used in this category of process monitoring algorithm. The calculation method is as follows

$$T^2 = t_{ns}^T \Lambda^{-1} t_{ns} \sim J_{th,T^2}(\frac{A(N^2-1)}{N(N-A)} F_\alpha(A, N-A)) \tag{9}$$

$$SPE = \|e\|^2 \sim J_{th,SPE}(g\chi^2_{\alpha,\tilde{h}}) \tag{10}$$

where $\Lambda = \frac{1}{N-1} T^T T$, $F_\alpha(A, N-A)$ denotes the F distribution follow the significance level α, and its degree of freedom is set as A and $N-A$. $g\chi^2_{\alpha,\tilde{h}}$ denotes the χ^2 distribution, which obeys $\tilde{h} = 2\overline{u}^2/S_\delta$ freedom of degree, $g = S/2\overline{u}$. $\overline{u}$ and S_δ are the sample mean and variance of *SPE*.

During this process, when T exceeds the threshold, a quality-related fault is considered to occur. When only the *SPE* statistic exceeds its threshold, a quality-unrelated fault is considered to occur.

The purpose of PLS is to decompose processssss variables into two completely orthogonal parts: quality-related and quality-unrelated.However, as can be seen from Formulas (6 and 7), it is obvious that $\hat{u}$ and e are not orthogonal to each other, which leads to the existence of parts irrelevant to KPIs in $\hat{u}$ and changes highly correlated to quality variables in e. Therefore, PLS model is not fully applicable to quality -related fault detection.

B. Improved principal component regression (IPCR)
PCA is a widely used method in the field of fault detection because of its ability to project high-dimensional data into low-dimensional latent variable space. But it is not suitable for practical industrial process because it is unable to identify whether the fault is related to quality. To solve this problem, a series of modified algorithms based on PCA are proposed. This part briefly introduces one of the improved algorithms called IPCR [15].

Execute the basic steps of PCA on U

1. Eigenvalues p and eigenvectors c are obtained by performing eigenvalue decomposition on $\frac{U^T U}{N-1}$, and they are collected to form matrices $P = [p_1 \ldots p_m]$ and $C = diag\{c_1, c_2, \ldots, c_m\}$ respectively.
2. The eigenvectors in P corresponding to the first A maximum eigenvalues of C are extracted to establish the load matrix $P = [p_1, \ldots, p_A]$.
3. Then $T = UP$

4. U is decomposed as follows

$$U = \hat{U} + \tilde{U} = TP^T + \tilde{U}$$

where T is the score matrix and $\tilde{U}$ represents the residual.

Considering that PCA is unable to identify whether the fault is related to quality, partial least squares regression is used to establish the relationship between T and Y. And in this way, the method, called IPCR, is used to detect quality-related failures.

$$Q^T = (T^T T)^{-1} T^T Y \tag{11}$$

$$\hat{Y} = TQ^T = UPQ^T = U\Upsilon \tag{12}$$

At this point, the relationship between U and Y is established, and Υ is the coefficient matrix.

PCR algorithm has a similar problem to PLS: it contains parts unrelated to quality in the principal component space, and changes related to quality exist in the residual space. In order to solve this problem, SVD is applied to further decompose the matrix $\Upsilon\Upsilon^T$.

$$\Upsilon\Upsilon^T = \begin{bmatrix} \Psi_\Upsilon & \tilde{\Psi}_\Upsilon \end{bmatrix} \begin{bmatrix} \Lambda_\Upsilon & 0 \\ 0 & 0 \end{bmatrix} \begin{bmatrix} \Psi_\Upsilon^T \\ \tilde{\Psi}_\Upsilon \end{bmatrix} \tag{13}$$

$$\Theta_\Upsilon = \Psi_\Upsilon \Psi_\Upsilon^T \in \mathbb{R}^{m \times m} \tag{14}$$

$$\Theta_\Upsilon^\perp = \tilde{\Psi}_T \tilde{\Psi}_\Upsilon^T \in \mathbb{R}^{m \times m} \tag{15}$$

where $\Psi_\Upsilon \in \mathbb{R}^{m \times s}$, $\tilde{\Psi}_\Upsilon \in \mathbb{R}^{m \times (m-s)}$ and $\Lambda_\Upsilon \in \mathbb{R}^{s \times s}$, Θ_Υ and $\Theta_\Upsilon^\perp$ are projection matrices that are orthogonal to each other. U is projected onto these two matrices and is represented as:

$$\hat{U} = U\Theta_\Upsilon = T_R \Psi_\Upsilon^T \in S_{\hat{U}} \equiv span\{\Upsilon\} \tag{16}$$

$$\tilde{U} = U\Theta_\Upsilon^\perp = T_U \tilde{\Psi}_\Upsilon^T \in S_{\tilde{U}} \equiv span\{\Upsilon\}^\perp \tag{17}$$

where $T_R = U\Psi \in \mathbb{R}^{N \times s}$ and $T_U = U\tilde{\Psi} \in \mathbb{R}^{N \times (m-s)}$ represent the score matrix of quality-related part $\hat{U}$ and quality-unrelated part $\tilde{U}$ respectively.

During the online detection process, an online sample u is available. According to the description above, the statistics are as follows:

$$t_R = \Psi^T x \in \mathbb{R}^{N \times m} \tag{18}$$

$$t_U = \tilde{\Psi}^T x \in \mathbb{R}^{m \times (s-m)} \tag{19}$$

$$x_r^T x_r = x^T \Psi_\Upsilon \Psi_\Upsilon^T \Psi_\Upsilon \Psi_\Upsilon^T x = t_r^T t_r \tag{20}$$

$$x_u^T x_u = x^T \tilde{\Psi}_\Upsilon \tilde{\Psi}_\Upsilon^T \tilde{\Psi}_\Upsilon \tilde{\Psi}_\Upsilon^T x = t_u^T t_u \tag{21}$$

Therefore, the T^2 statistic for the quality-related part and the quality-unrelated part:

$$T_R^2 = t_R^T (\frac{T_R^T T_R}{N-1})^{-1} t_R \tag{22}$$

$$T_U^2 = t_U^T (\frac{T_U^T T_U}{N-1})^{-1} t_U \tag{23}$$

According to the significance level α, the thresholds are as follows:

$$J_{th,T_R^2} = \frac{m(N^2-1)}{N(N-m)} F_\alpha(m, N-m) \tag{24}$$

$$J_{th,T_U^2} = \frac{(s-m)(N^2-1)}{N(N-m)} F_\alpha(s-m, N-s+m) \tag{25}$$

According to fault detection logic:

$T_R^2 > J_{th,T_R^2} \Rightarrow$ A quality-related fault has occurred
$T_U^2 > J_{th,T_U^2} \Rightarrow$ A quality -unrelated fault has occurred

3 The Proposed Method

A. Regression Partial Least Squares (RPLS)
To solve the problem of PLS oblique decomposition of process space, a new fault detection method named Regression partial least squares (RPLS) was proposed in this part.

Traditional PLS algorithm decomposed the process variable space U into the following form.

$$\begin{aligned} U &= TP^T + E = \hat{U} + \tilde{U} \\ Y &= TQ^T + F = \hat{Y} + \tilde{Y} \\ T &= UR \end{aligned} \tag{26}$$

T is reproject to $T_y T_y$

$$T_y = \hat{Y} Q_y = TQ^T Q_y = TM \tag{27}$$

where M is the projection matrix of T.Then, least square regression is carried out between T_y and $\hat{U}$ to get Ψ_y.

$$\Psi_y^T = (T_{\text{yrpls}}^T T_{\text{yrpls}})^{-1} T_{\text{yrpls}}^T \hat{U} \tag{28}$$

Reference formula (29)

$$U_y = T_{\text{yrpls}} \Psi_y^T = T_{\text{yrpls}} (T_{\text{yrpls}}^T T_{\text{yrpls}})^{-1} T_{\text{yrpls}}^T TP^T \tag{29}$$

$$U_u = U - U_y \tag{30}$$

where U_y and U_u are the parts that are highly correlated and independent of Y, respectively. The process variable space U is reconstructed during the above procedure.

The T^2 statistic is used to monitor both parts. PCA is performed on KPI-unrelated part U_u to obtain its score matrix T_u and the loading matrix P_u.

Lemma 1. After the decomposition of RPLS, U_u is completely unrelated to $\hat{Y}$.

Proof

According to formula (31):

$$U_u = U - U_y = (I - T_{yrpls}(T_{yrpls}^T T_{yrpls})^{-1} T_{yrpls})U \tag{31}$$

Then

$$T_{yrpls}^T U_u = (T_{yrpls}^T - T_{yrpls}^T T_{yrpls}(T_{yrpls}^T T_{yrpls})^{-1} T_{yrpls})U = 0 \tag{32}$$

T_{yrpls} is the score matrix obtained by PCA decomposition of $\hat{Y}$, so

$$\hat{Y} = T_{yrpls} Q_y^T = 0 \tag{33}$$

$$\hat{Y} U_u = T_{yrpls} Q_y^T U_u = 0 \tag{34}$$

It can be inferred that U_u is not related to $\hat{Y}$, the proof is complete.

For online processes, a new online sample u_{new} is available. Its score t_{new} can be given by

$$t_{new} = u_{new}^T P \tag{35}$$

Therefore, the score of the online sample can be calculated by the following formula

$$t_{ynew} = t_{new}^T Q^T Q_y = u_{new}^T PM \tag{36}$$

Thus, the score of quality-unrelated part can be expressed as formula (37)

$$t_{unew}^T = u_{unew}^T P = (u_{new}^T - t_{ynew}^T \Psi_y^T) P_u = (u_{new}^T - u_{new}^T PM \Psi_y^T) P_u \tag{37}$$

Considering the large variances of the two parts, quality-related and quality-unrelated T^2 statistic was selected for monitoring:

$$T_y^2 = t_{ynew}^T \left(\frac{T_y^T T_y}{N-1}\right)^{-1} t_{ynew} \tag{38}$$

$$T_u^2 = t_{unew}^T \left(\frac{T_u^T T_u}{N-1}\right)^{-1} t_{unew} \tag{39}$$

B. An adaptive threshold based on Exponentially Weighted Moving Average

Generally speaking, the fault detection methods based on multivariate statistics adopt the method of fixed control limit to set the threshold α. The control limit is generally determined by the confidence level. This method balances the relationship between false alarm rate and false alarm to a certain extent. According to the algorithm model, the T^2 statistic $T^2 = [t_1, t_2..., t_i]$ is obtained. When the statistic exceeds the threshold, the fault is considered to occur, that is, $t_i > J_{th}$. However, this method leads to a certain degree of false positives and missing positives, and is not sensitive to some specific types of faults.

In order to solve this problem, the exponential weighted moving average (EWMA) method is applied to improve the threshold. The core idea of the improved method is a moving average weighted by exponential decline, and the weight of each value decreases exponentially with time. The closer the data is to the current moment, the greater the weight. Based on this idea, the adaptive threshold at time i is:

$$\mathrm{t}_i = \frac{\sum_{j=1}^{h} \lambda^j t_{i-h+j}}{\sum_{j=1}^{h} \lambda^j} = \frac{\lambda t_{i-h+1} + \lambda^2 t_{i-h+2} + ... + \lambda^h t_i}{\sum_{j=1}^{h} \lambda^j} \tag{40}$$

However, as this is a reverse summation method, the detection time for the handoff between normal data and abnormal data will be prolonged due to its hysteresis. To solve this problem, a new method, such as Eq. (41), is proposed.

$$\mathrm{t}_i = \frac{(J_{th} \sum_{j=1}^{h} \lambda^j - \sum_{j=1}^{h-1} \lambda^j t_{i-h+j})}{\lambda^h} \tag{41}$$

This method combines two parts. The first part is the change of the traditional fixed threshold upper limit under a certain confidence level. The second part also considers the deviation of the previous non alarm samples, which is more suitable for setting the appropriate adaptive threshold according to the real-time samples. However, due to the cumulative effect of previous error samples, the adaptive threshold may be lower than the conventional level, which affects the normal detection effect. Therefore, a certain lower limit [20] can be set by Eq. (42) to improve this problem.

$$J_{thirpls} = \max \left\{ \frac{(J_{th} \sum_{j=1}^{h} \lambda^j - \sum_{j=1}^{h-1} \lambda^j t_{i-h+j})}{\lambda^h}, \frac{J_{th}}{2} \right\} \tag{42}$$

In this article, a fault is considered to have occurred when a statistic exceeds a threshold. In the above formula, the selection of weighting factor should be able to ensure that the most recent statistics are close to the healthy sample. The closer the weighting factor is to 1, the more false alarm can be reduced. However, problems similar

to Formula (41) will also occur, leading to a high detection time delay, which is not suitable for intermittent fault detection. If the weight factor is too high, it will lead to too much correlation with the recent data. Although the detection time can be reduced, the ability of the algorithm itself to eliminate the cumulative effect will be reduced, and the detection rate will be indirectly reduced. The window length h represents the number of samples to be considered for setting the adaptive threshold. First of all, sufficient numbers are needed to ensure the credibility of the adaptive threshold. On the other hand, an excessively large h will cause the weight factor of the sample farthest from the current moment to be too small and ignored compared with the weight of the sample at the recent moment, losing the significance of adding this part of the sample to the formula.

In this part, the adaptive threshold is applied to PLS and IPCR algorithm instead of the original fixed threshold. The thresholds of PLS in Eqs. 9 and 10 are replaced by the following:

$$J_{thpls} = \max\left\{\frac{(J_{th,T^2}\sum_{j=1}^{h}\lambda^j - \sum_{j=1}^{h-1}\lambda^j t_{i-h+j})}{\lambda^h}, \frac{J_{th,T^2}}{2}\right\} \tag{43}$$

$$J_{thpls} = \max\left\{\frac{(J_{th,SPE}\sum_{j=1}^{h}\lambda^j - \sum_{j=1}^{h-1}\lambda^j t_{i-h+j})}{\lambda^h}, \frac{J_{th,SPE}}{2}\right\} \tag{44}$$

The thresholds of PLS in Eqs. 24, 25 and 26 are replaced by the following:

$$J_{thipcr} = \max\left\{\frac{(J_{th,T_R^2}\sum_{j=1}^{h}\lambda^j - \sum_{j=1}^{h-1}\lambda^j t_{i-h+j})}{\lambda^h}, \frac{J_{th,T_R^2}}{2}\right\} \tag{45}$$

$$J_{thipcr} = \max\left\{\frac{(J_{th,T_U^2}\sum_{j=1}^{h}\lambda^j - \sum_{j=1}^{h-1}\lambda^j t_{i-h+j})}{\lambda^h}, \frac{J_{th,T_U^2}}{2}\right\} \tag{46}$$

In the TE [21] process, the feed temperature of reactant C is changed to simulate a quality-related fault condition to verify the effectiveness of the adaptive threshold.

Figure 1 and Fig. 2 show the fault detection results of PLS and IPCR using traditional fixed threshold and adaptive threshold respectively. The solid black line represents the traditional fixed threshold, while the solid red line represents the adaptive threshold. It is clear that the red line in Fig. 1 is lower than the black line in most cases in both the quality-related subspace and the quality-unrelated subspace, which means that the PLS

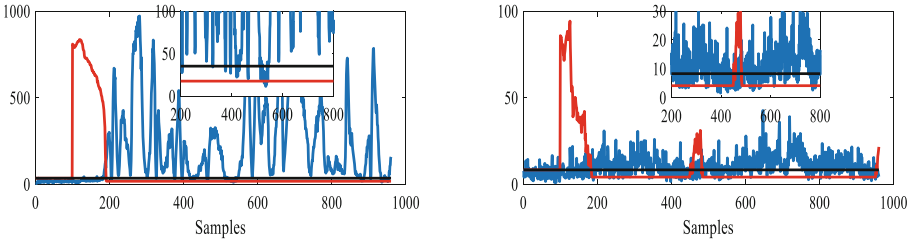

Fig. 1. Fault detection chart of modified PLS

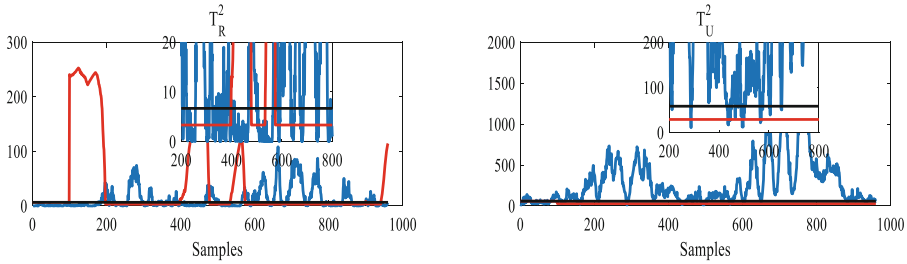

Fig. 2. Fault detection chart of modified IPCR

using the adaptive threshold can provide more alarm than the PLS using the traditional fixed threshold. In Fig. 2, IPCR using the adaptive threshold provides more alerts in the quality-unrelated subspace than the method using the fixed threshold. In the quality-related subspace, the statistics of the part where the red line is higher than the black line fail to exceed the threshold, indicating that this part of the fault has not been detected by IPCR and does not affect the validity of the verification of the adaptive threshold. Through this part of work, the validity of the adaptive threshold is verified.

C. IRPLS algorithm flow

The specific process based on IRPLS algorithm is as follows. Steps 1 to 6 are offline training, and steps 7 to 10 are online monitoring:

Offline Model Training:

Step 1: Normalize the input matrices X and output matrices Y.

Step 2: Establish PLS model by using input/output matrix.

Step 3: Perform PCA on the quality variables Y of the PLS model to get the score matrix T_{yrpls}.

Step 4: The load matrix Ψ_y is obtained by performing least square regression on X and T_{yrpls}.

Step 5: Calculate the quality-related U_y and quality-unrelated parts U_u according to Eqs. (29) and (30).

Step 6: Perform PCA on the quality- unrelated part U_u to get the corresponding score T_u and load matrix P_u.

On-line Monitoring:

Step 7: For an online sample u, score t_{ynew} and t_{unew} of quality-related and quality-unrelated parts were calculated by using Eqs. (34–36).
Step 8: Calculate the statistics T_y^2 and T_u^2 of the two subspaces according to the formulas (38–39).
Step 9: According to formula (42), the adaptive threshold is set in the following form

$$J_{thirpls} = max\left\{\frac{(J_{th}\sum_{j=1}^{h}\lambda^j - \sum_{j=1}^{h-1}\lambda^j t_{i-h+j})}{\lambda^h}, \frac{J_{th,T_y^2}}{2}\right\} \tag{47}$$

$$J_{thirplsun} = max\left\{\frac{(J_{th}\sum_{j=1}^{h}\lambda^j - \sum_{j=1}^{h-1}\lambda^j t_{i-h+j})}{\lambda^h}, \frac{J_{th,T_u^2}}{2}\right\} \tag{48}$$

Step 10: According to the fault detection logic to monitor the fault and determine whether the fault is related to quality.
$T_y^2 > J_{thirpls} \Rightarrow$ A quality-related fault was detected in quality-related subspace
$T_u^2 > J_{thirplsun} \Rightarrow$ A quality-unrelated fault detected in quality-unrelated subspace
$T_y^2 < J_{thirpls}$ and $T_u^2 < J_{thirplsun} \Rightarrow$ No fault detected

In order to clarify the algorithm steps, the process of IRPLS algorithm is presented here, as shown in Fig. 3.

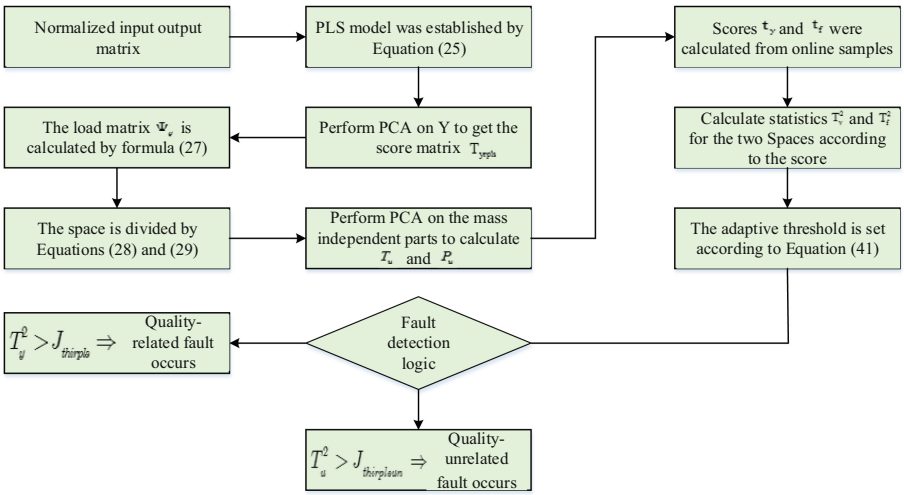

Fig. 3. Algorithm flow chart

4 Numerical Case Simulation

In this module, a linear numerical case and a nonlinear numerical case are used to simulate and compare the three algorithms of PLS, IPCR and IRPLS to reflect the effectiveness of the algorithm. FDR is introduced as a performance index to evaluate the algorithm.

$$FDR = \frac{N_{\mathrm{r}}}{N_{\mathrm{t}}} \tag{49}$$

where N_{t} is the total number of samples, and N_{r} is the number of effective alarms.

An excellent algorithm that can be applied in industrial practice should be equipped with the following capabilities:

a) For quality-related faults: There are as many alerts as possible in the quality- related subspace and quality- unrelated subspace;
b) For quality-unrelated faults: There are as few or no alerts as possible in the quality-related subspace, and as many alerts as possible in the quality- unrelated subspace.

A. Linear numerical case

In order to verify the effectiveness of the method proposed in this paper, a widely circulated linear numerical case [9] is used here to simulate and verify PLS, IPCR and IRPLS. The case model description is shown in Eq. (50).

$$\begin{cases} u_l = Bz_l + e_l \\ y_l = \Xi u_l + v_l \end{cases} \tag{50}$$

$$B = \begin{bmatrix} 1 & 3 & 4 & 4 & 0 \\ 3 & 0 & 1 & 4 & 1 \\ 1 & 1 & 3 & 0 & 0 \end{bmatrix}^T \quad e_l \in \mathbb{R}^5 \quad u_l = [u_{l,1}\ u_{l,2}\ u_{l,3}\ u_{l,4}\ u_{l,5}]^T$$

$$\Xi = [2\,2\,1\,1\,0] \qquad u_l = N(0, 0.01^2)$$

in which $z_l \in \mathbb{R}^3$, $z_{l,i} \sim U([0, 1])(i = 1, 2, 3)$, $e_{l,j} \sim N(0, 0.05^2)(j = 1, 2, 3, 4, 5)$. In this case, the fault is introduced into the sample in the following form:

$$u_l = u_l^* + \Theta f$$

u_l is the failure-free value,Θ and f represent the direction and magnitude of fault, respectively.

In this part, 400 normal samples were used to model the PLS, IPCR and IRPLS algorithms, and another 400 samples were introduced to test the model performance $\lambda = 1.06$, $h = 50$. The fault is introduced in the last 200 samples, and the fault scenario is as follows:

Failure Scenario 1: The fault direction is set to $\Theta = [0\,0\,0\,0\,1]$

$$y_l = \Xi(u_l^* + \Theta f) = \Xi u_l^* + \Xi\Theta f = \Xi u_l^*$$

It is clear that y is not affected by f, so this kind of failure scenario is quality-unrelated.

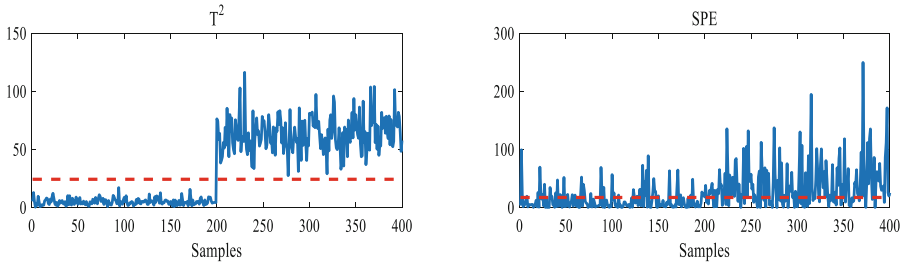

Fig. 4. PLS detection diagram for Failure Scenario 1 when f = 4

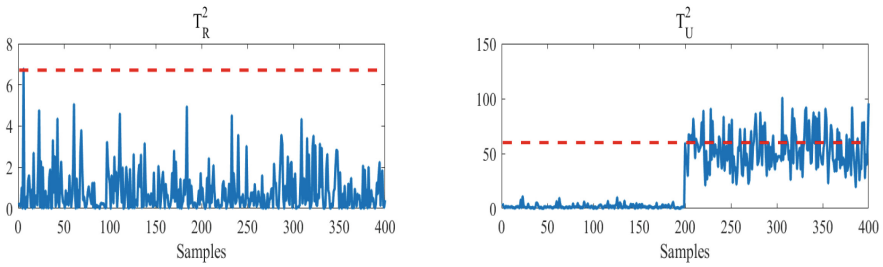

Fig. 5. IPCR detection diagram for Failure Scenario 1 when f = 4

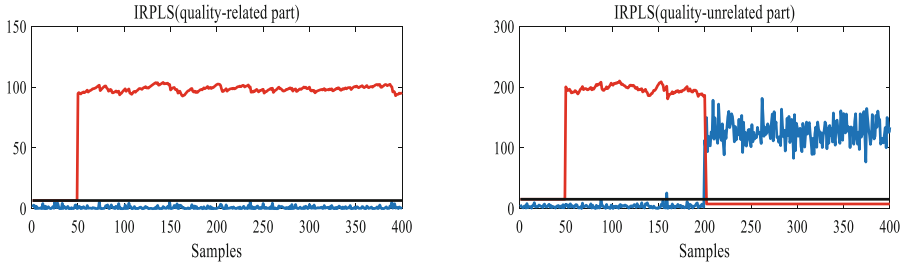

Fig. 6. IRPLS detection diagram for Failure Scenario 1 when f = 4

Figures 4, 5 and 6 are the detection diagrams of PLS, IPCR and IRPLS for fault scenario 1 when the fault intensity is 4, respectively. In Figs. 4, 5, PLS misjudged this quality-unrelated as a quality-related fault, while IPCR failed to detect such a fault scenario in quality-unrelated subspace. In Fig. 6, the solid black line represents RPLS algorithms using traditional thresholds, and the solid red lines represent IRPLS algorithms using adaptive thresholds. It can be seen that the red line in the quality-unrelated subspace is lower than the black line, indicating that for quality-unrelated faults, IRPLS algorithm can provide a higher fault detection rate than RPLS algorithm. So it is obvious that the adaptive threshold is valid in RPLS and IRPLS is more consistent with the fault detection logic than the other three algorithms.

Table 1 shows the FDRs of the three methods for the fault scenario 1 under different fault intensities. It can be seen that PLS has a good detection effect on quality-unrelated

faults in the residual subspace, but it also generates a large number of alerts in the principal component space, which is not consistent with the actual situation. In general, when the fault magnitude is intense, both IPCR and IRPLS can give as few alarms as possible in the quality-related space and as many alarms in the quality-unrelated subspace, which is in line with the fault detection logic. However, it is worth noting that when the fault intensity is low, IPCR has a small number of false alarms in the quality-related subspace, and it also provides insufficient alarm rate in the quality-unrelated subspace. However, IRPLS does not have false positives in the quality-related subspace. When the fault level is at a low level, the alarm rate of IRPLS in the quality-unrelated subspace is more than 80%, and quickly reaches 100% with the increase of fault intensity. Therefore, the detection ability of IRPLS for linear quality-unrelated faults is higher than PLS and IPCR.

Table 1. FDRs of fault scenario 1 under different fault intensities

Fault magnitude	PLS		IPCR		IRPLS	
	T^2	SPE	T_R^2	T_U^2	T_y^2	T_u^2
2	0.285	0.45	0.005	0	0	0.88
4	1	0.89	0.01	0.265	0	0.99
6	1	1	0.005	0.97	0	1
8	1	1	0	1	0	1
10	1	1	0	1	0	1

Failure Scenario 2: The fault direction is set to $\Theta = [22110]$

$$y_l = \Xi(u_l^* + \Theta f) = \Xi u_l^* + \Xi\Theta f \neq \Xi u_l^*, \forall f \neq 0$$

It can be seen that y is affected by f and its fault level in this kind of fault, so this kind of failure scenario is identified as quality-related fault.

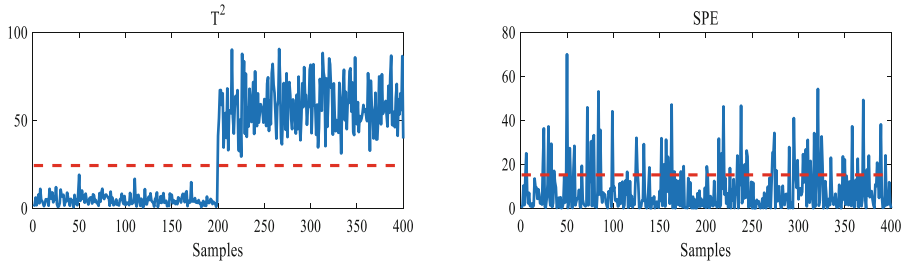

Fig. 7. PLS detection diagram for Failure Scenario 2 when f = 6

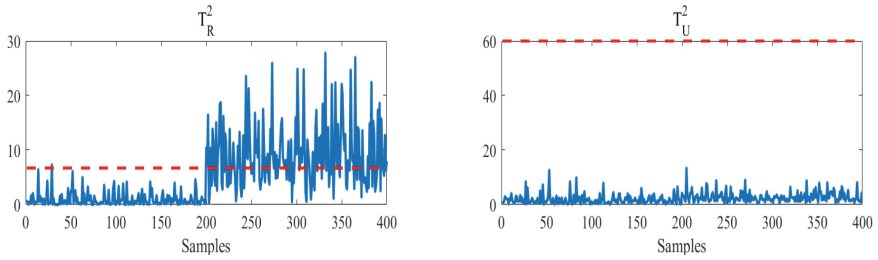

Fig. 8. IPCR detection diagram for Failure Scenario 2 when f = 6

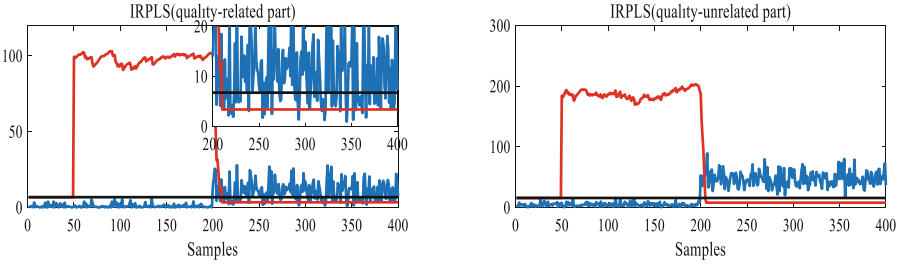

Fig. 9. IRPLS detection diagram for Failure Scenario 2 when f = 6

Figure 7, 8 and 9 are the detection diagrams of PLS, IPCR and IRPLS for fault scenario 2 when the fault intensity is 6, respectively. It can be seen that the alarm of IRPLS in quality-related subspace exceeds that of PLS and IPCR, which is more in line with the actual situation. In addition, the red line in Fig. 9 is lower than the black line, so the alarm rate of IRPLS is also higher than that of RPLS.

Table 2. FDRs of fault scenario 2 under different fault intensities

Fault magnitude	PLS		IPCR		IRPLS	
	T^2	SPE	T_R^2	T_U^2	T_y^2	T_u^2
2	0	0.56	0.055	0	0	0
4	0.17	0.805	0.23	0	0.055	0
6	0.815	0.585	0.73	0	0.865	0.935
8	1	1	0.885	0	0.985	0.975
10	1	1	1	0	0.995	1
20	1	1	1	0	1	1

Table 2 shows the detection rates of quality-related faults by PLS, IPCR and IRPLS methods under different fault intensities. It can be seen that when the fault is at a lower level, the detection capabilities of PLS, IPCR and IRPLS all need to be improved.

With the gradual increase of fault intensity, the performance differences of these three fault detection methods appear. When the fault intensity rises to 6, the detection ability of IRPLS begins to exceed that of PLS and IPCR. It can be concluded that IRPLS outperforms PLS and IPCR in terms of linear quality related fault detection.

B. Nonlinear numerical case

In this section, a nonlinear numerical case [11] is introduced to verify the performance of the three algorithms in the nonlinear system. The specific model is described as follows:

$$u_1 \sim N(1, 0.01^2), u_2 \sim N(1, 0.01^2) \tag{51}$$

$$u_3 = \sin(u_1) + d_1 \tag{52}$$

$$u_4 = u_1^2 - 3u_1 + 4 + d_2 \tag{53}$$

$$u_5 = u_2^2 + \cos(u_2^2) + 1 + d_3 y = u_3^2 + u_3 u_4 + u_1 + o \tag{54}$$

where $d_j \sim N(0, 0.001^2)(j = 1, 2, 3)$, $o \sim N(0, 0.005^2)$.

It can be seen that variables 1, 3 and 4 are directly or indirectly related to quality indicator y, and faults occurring in them are considered as quality-related faults. Variables 2 and 5 are not related to y, so the failures occurring in them are considered to be quality-unrelated.

In this experiment, 960 normal data were selected to establish PLS, IPCR and IRPLS models, and 960 test data were used to verify the model performance of these methods. Window length $h = 100$, weighting factor $\lambda = 1.06$. The fault is introduced in the 481st sample. The fault is set as the following four forms, and the fault level is $f = 0.1$, $f = 0.001, f = 1$ and $f = 0.01$ respectively.

Failure Scenario 1:$u_2 = u_2^* + f$
Failure Scenario 2: $u_2 = u_2^* + (i - 480)f$
Failure Scenario 3: $u_1 = u_1^* + f$
Failure Scenario 4: $u_1 = u_1^* + (i - 480)f$

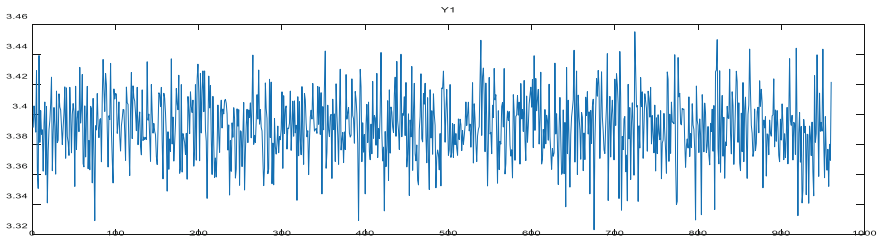

Fig. 10. Quality monitoring diagram for Failure Scenario 1 when f = 1

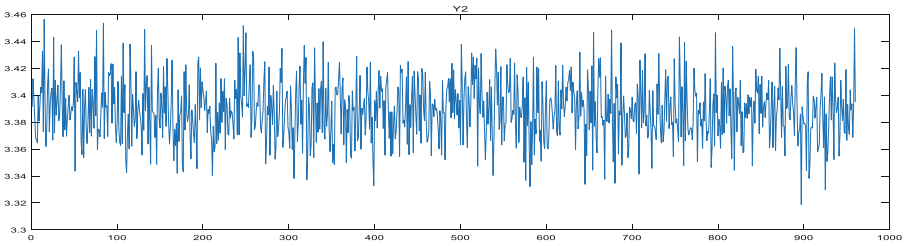

Fig. 11. Quality monitoring diagram for Failure Scenario 2 when f = 10

Figure 10 and Fig. 11 are the quality monitoring charts for quality-unrelated failure scenarios 1 and 2 at different levels. It can be seen that when these two faults occur and the grade changes, the quality does not change, so it can be inferred that these two faults are quality-independent faults.

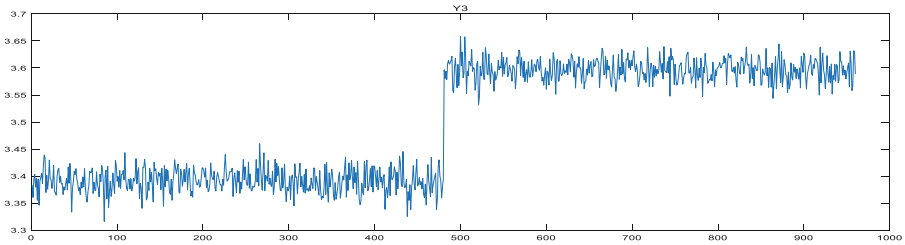

Fig. 12. Quality monitoring diagram for Failure Scenario 3 when f = 1

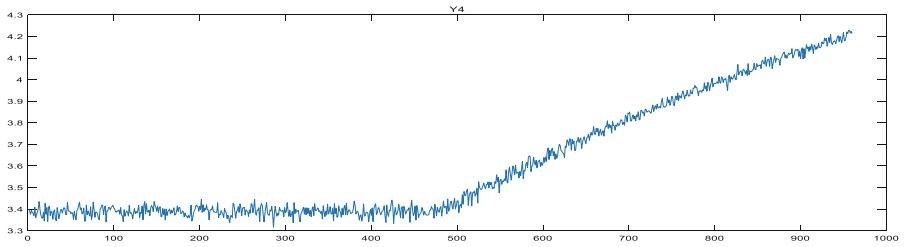

Fig. 13. Quality monitoring diagram for Failure Scenario 4 when f = 1

Figures 12, 13 are the quality monitoring charts for quality-related failure scenarios 3 and 4 at different intensities. As you can see, the quality changes rapidly after these two types of faults occur, so fault scenarios 3 and 4 bit quality-related failures.

According to the above analysis, the failure scenarios 1 and 2 are quality-unrelated faults, while the fault scenarios 3 and 4 are quality-related faults. The four fault levels are set as tiny levels to verify the ability of the algorithm to detect minor faults in nonlinear systems.

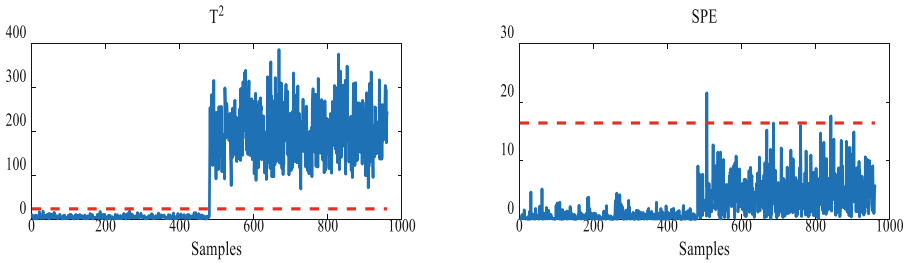

Fig. 14. PLS detection diagram for Failure Scenario 1 when f = 1

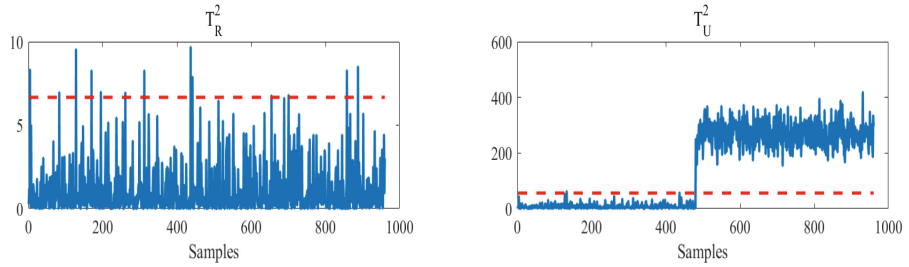

Fig. 15. IPCR detection diagram for Failure Scenario 1 when f = 1

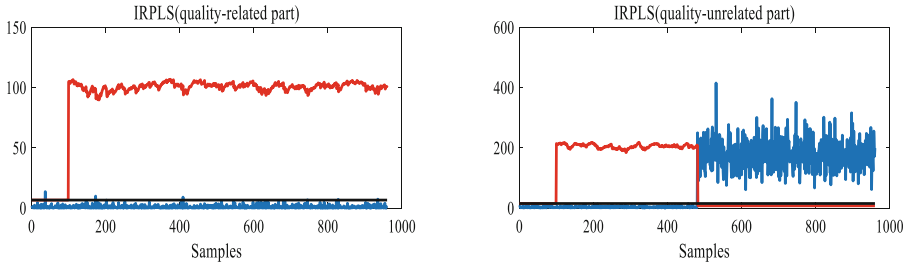

Fig. 16. IRPLS detection diagram for Failure Scenario 1 when f = 1

Figures 14, 15 and 16 are the detection diagrams of PLS, IPCR and IRPLS for fault scenario 1 when the fault intensity is 1, respectively. As can been seen, all three methods are completely alert in the quality-unrelated subspace. However, PLS misjudged this

kind of fault as a quality-related fault by a large number of alarms in the quality-related subspace, which was not in line with the actual situation. While IPCR had a small number of false positives and IRPLS had no false positives.

Table 3. FDRs of different fault scenarios under different fault intensities

Fault Scenario	Type	magnitude	PLS		IPCR		IRPLS	
			T^2	SPE	T_R^2	T_U^2	T_y^2	T_u^2
1	Step	0.1	1	0	0.0083	1	0	1
2	ramp	0.001	0.9125	0.65	0.0104	0.9063	0	0.9146
3	Step	1	1	1	1	1	1	1
4	ramp	0.01	0.9875	0.973	0.9700	0.9700	0.9875	0.9813

Table 3 shows the fault detection rates of PLS, IPCR and IRPLS for four fault scenarios under different fault intensities. Obviously, for the quality-unrelated fault scenario 1 and scenario 2, the false positive rate of IRPLS algorithm in the KPI-related subspace is 0, and both PLS and IPCR have different degrees of false positive. The alarm rate of IRPLS in the quality-related subspace is also higher than that of PLS and IPCR. For quality-related fault scenarios 3 and 4, IRPLS still has the highest alarm rate in the quality-related subspace. In summary, IRPLS has the most superior detection results for non-linear and minor faults.

C. Tennessee process simulation
The TE model is set up by the Eastman Chemical Company, which are widely used to validate the property of process monitoring methods [22], the specific reaction process is as shown in Fig. 17.

The process is composed of reactor, condenser, compressor, separator and stripper. In this process, four gas components A, C, D, E and an inert component B participate in the reaction to generate two liquid main products G and H and a liquid by-product F. The reaction is closed-loop and irreversible, and the reaction process can be expressed as follows

$$\begin{aligned} &A + C + \mathrm{D}\ (E) \rightarrow \mathrm{G}\ (H) \\ &A + E \rightarrow F \\ &3D \rightarrow 2F \end{aligned} \tag{55}$$

The whole process is divided into two parts. The first part consists of 41 measurement variable modules, which are further divided into 22 continuous process variables (XMEAS (1–22)) and 19 analytical variables (XMEAS(23–41)), and the second part consists of 12 operational variable modules (XMV(1–12)).In general, 11 operational variables and 22 continuous process variables are selected to construct the input matrix. The module representing the final product G or H can be used as the quality variable, and the sampling interval is 3 min.

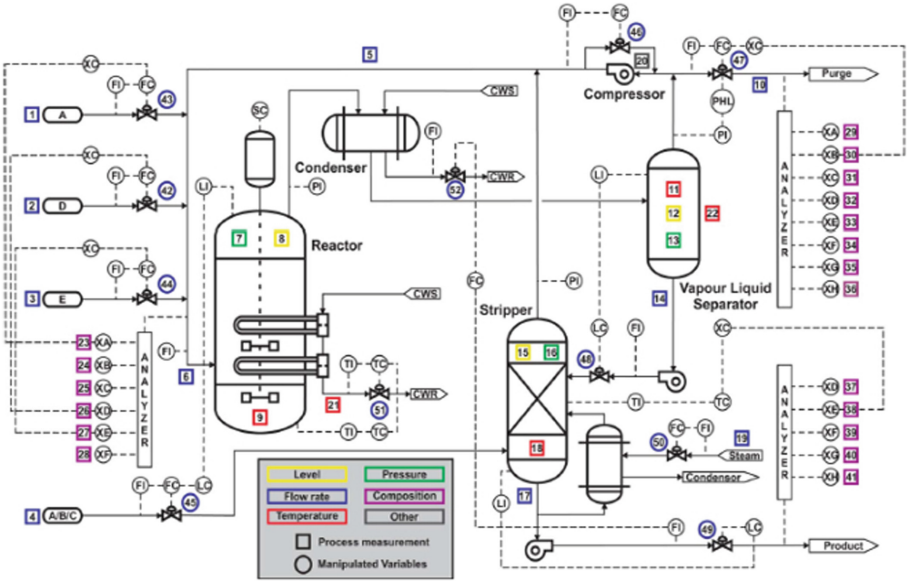

Fig. 17. TE Process Flowchart

21 faults were set in the TE process, including 15 known faults and 6 unknown faults [9]. The data set including a total of 22 training sets and the same number of test sets corresponding to the corresponding fault and one fault-free case under normal working conditions, which were collected within 48 h of operation time, and were widely used in the field of process monitoring [23]. In order to verify 15 kinds of known faults, this paper selects data sets corresponding to faults and data sets under fault-free conditions for simulation verification. The number of samples in the training set and the number of samples in the test set are 480 and 960 respectively, and the number of modeling training collected under normal working conditions is 500.In this paper, the failure was introduced after the 160th sample.

Figure 18 shows the detection rate of IRPLS algorithm for different quality-related faults with different weighting factors. It can be seen that when the weighting factor is 1.06, the fault detection rate is generally the highest, so in the TE model: $\lambda = 1.06$, $h = 100$.

According to prior knowledge, 15 known fault types are divided into quality-related fault (IDV(1), IDV(2), IDV(6), IDV(8), IDV(10), IDV(12), IDV(13)) and quality-unrelated fault (IDV(3), IDV(4), IDV(9), IDV(11), IDV(14), IDV(15)). As shown in Fig. 19, after the occurrence of fault IDV (14), the trend of quality variable is similar to that under normal working conditions without significant changes, which also proves that IDV(14) is quality-unrelated fault. Figures 20, 21 and 22 are the detection diagrams of PLS, IPCR and IRPLS for quality-unrelated faults IDV(14) respectively. It is obvious that both PLS and IPCR have varying degrees of alarm in the quality-related subspace, which does not help us identify the correct type of fault. However, in Fig. 22, IRPLS

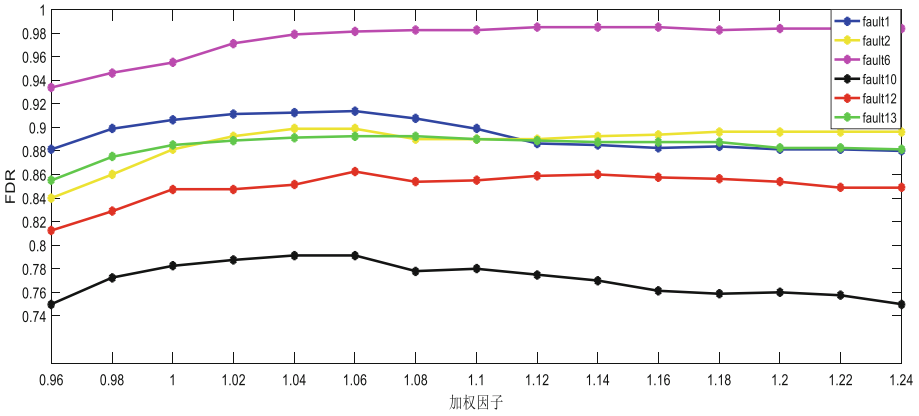

Fig. 18. FDRs of IRPLS under different weighting factors

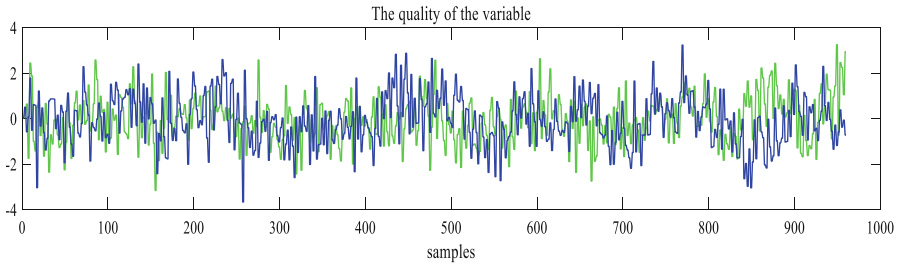

Fig. 19. Changes of molar ratio under different working conditions

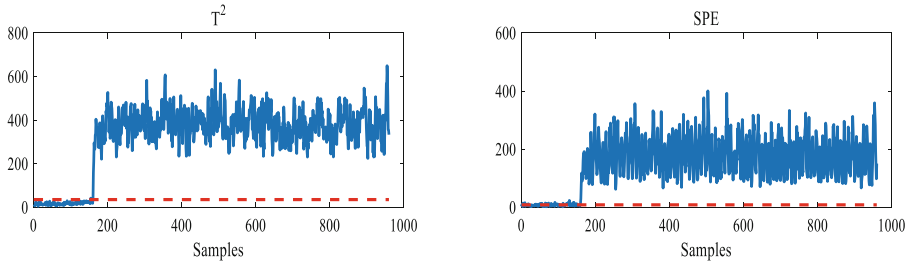

Fig. 20. PLS detection diagram for IDV(14)

only alerts in quality-related subspace and does not alarm in quality-unrelated subspace, indicating that IDV (14) is quality-unrelated fault.

FAR is introduced to evaluate the performance of the algorithm together with FDR:

$$FAR = \frac{N_w}{N_t} \tag{56}$$

where N_t is the total number of samples, and N_w is the number of false alarms.

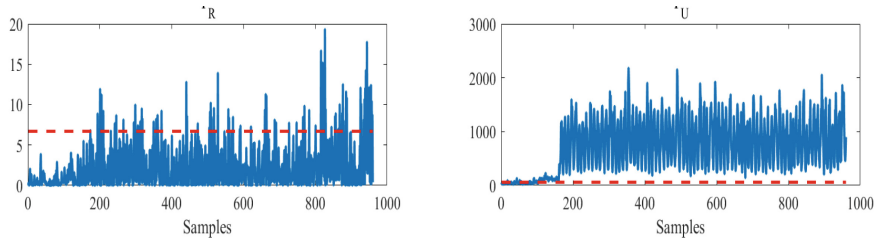

Fig. 21. IPCR detection diagram for IDV(14)

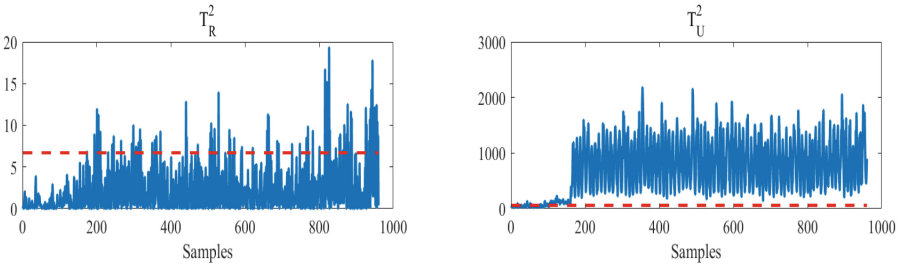

Fig. 22. IRPLS detection diagram for IDV(14)

Table 4 and Table 5 show the FDRs of quality-related faults and the FARs of quality-unrelated faults by the three methods respectively. As can be seen in Table 4, the detection ability of IPCR for fault 8 and fault 10 is slightly insufficient, while IRPLS and PLS have no obvious short board, which can provide a lot of alarms for all quality-related faults detected. Table 5 illustrates that IRPLS has the lowest far and the KPI-unrelated fault detection performance is the best. And for some faults such as IDV (3), IDV (14),IRPLS can achieve zero false alarm. In addition, it is worth mentioning that the high FAR of PLS for quality-unrelated faults means that it will misjudge quality-related faults as quality-related faults, which reduces the credibility of PLS for FDR of quality-related faults. It can be concluded that IRPLS has the highest FDR for quality-related faults and the lowest FAR for quality-unrelated faults.

Table 4. FDRs of quality-related faults

Fault ID	Fault Description	Fault detection rate		
		PLS	IPCR	IRPLS
1	A/C Feed Ratio, B Composition constant	0.9988	0.9063	0.9138
2	B composition A/C Ration Constant	0.9863	0.8838	0.8988
6	A Feed Loss Step	1	0.9913	0.9813

(*continued*)

Table 4. (*continued*)

Fault ID	Fault Description	Fault detection rate		
		PLS	IPCR	IRPLS
8	A, B, C Feed composition	0.985	0.6788	0.7925
10	C Feed temperature	0.8913	0.46	0.7850
12	condenser cooling water inlet temperature	0.9950	0.8413	0.8525
13	Reaction kinetics	0.9538	0.9038	0.8925

Table 5. FARs of quality-unrelated faults

Fault ID	Fault Description	Fault alarm rate		
		PLS	IPCR	IRPLS
3	D Feed Temperature (step)	0.0938	0.1363	0
4	Reactor cooling water inlet temperature	1	0.11	0.045
9	D Feed temperature (Random variation)	0.0663	0.075	0.005
11	Reactor cooling water inlet temperature	0.8213	0.1025	0.0413
14	Reactor cooling water valve	1	0.1	0
15	Condenser cooling water valve	0.16	0.105	0.0838

In addition, there is a class of known faults named regression faults, such as faults 5 and 7.After this kind of fault occurs, the feedback mechanism inside the system will be adjusted quickly to make the quality return to normal within a certain period of time. Whether this process can be monitored can reflect the following of the algorithm.

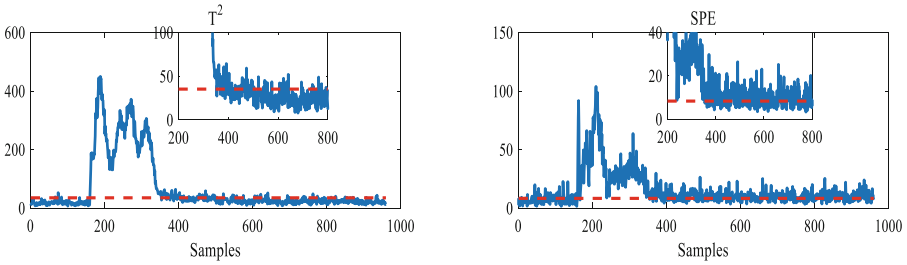

Fig. 23. PLS detection diagram for IDV (5)

Figure 26 shows the variation of the molar ratio of component G in stream 9 under different conditions. The blue solid line is the quality under normal conditions, and the green solid line is the quality under fault 5 conditions. It can be seen that the quality returns to normal after 400 samples. As can be seen from Fig. 25, IRPLS first gives a large

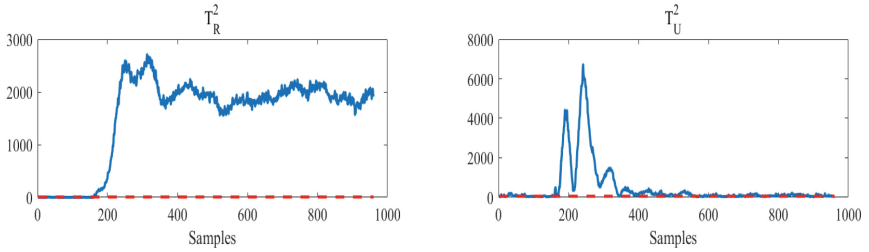

Fig. 24. IPCR detection diagram for IDV (5)

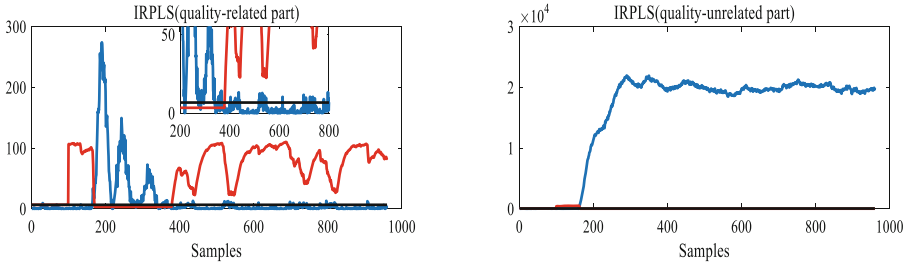

Fig. 25. IRPLS detection diagram for IDV (5)

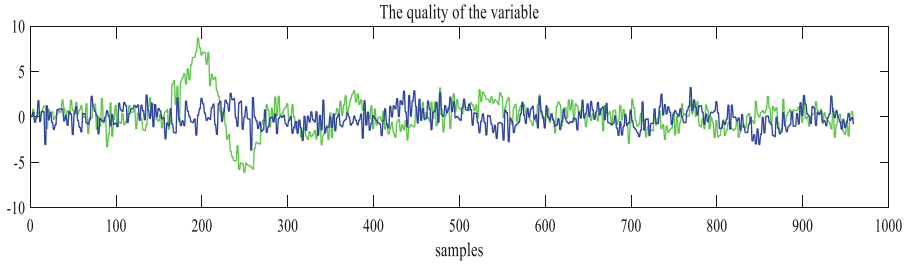

Fig. 26. Diagram of molar ratio change of component G in stream 9

number of alarms in the quality-related subspace, and then returns to normal quickly without any alarms. The presence of this fault can also be continuously monitored in the quality-unrelated subspace. However, neither Fig. 23 representing PLS nor Fig. 24 representing IPCR can give practical decisions. It can be concluded that IRPLS is better than PLS and IPCR in detecting regressive faults, and has stronger following ability, which is more suitable for industrial practice.

5 Conclusion

A quality-related fault detection method named IRPLS is proposed in this paper. In this method, the quality variables are decomposed and the relationship between the quality variables and the process variable space is established to reconstruct the process

variables so as to better describe the quality variables. Corresponding test statistics are designed and compared with the introduced adaptive thresholds to help produce more reliable decisions, which improves the shortcomings of standard PLS in the detection of quality-related faults. By comparing with PLS and IPCR in numerical examples and TE processes, it is concluded that IRPLS has higher detection accuracy for quality-related and quality-unrelated faults as well as minor faults, and has the best tracking performance for specific types of faults, which means it is more suitable for modern industrial processes.

Funding. This works is partly supported by the Education Committee Project of Liaoning, China under Grant LJKZ1011 and LJ2019003.

References

1. Qin, S.J.: Statistical process monitoring: basics and beyond. J. Chemometr. **17**(8–9), 480–502 (2003)
2. Liang, S., Zhang, S., Huang, Y., et al.: Data-driven fault diagnosis of FW-UAVs with consideration of multiple operation conditions. ISA Trans. **126**, 472–485 (2022)
3. Rezamand, M., Kordestani, M., Carriveau, R., et al.: A new hybrid fault detection method for wind turbine blades using recursive PCA and wavelet-based PDF. IEEE Sens. J. **20**, 2023–2033 (2020)
4. Pandit, R., Infield, D., Dodwell, T.: Operational variables for improving industrial wind turbine yaw misalignment early fault detection capabilities using data-driven techniques. IEEE Trans. Inst. Meas. **70**, 1–8 (2021)
5. Wang, K., Chen, J., Song, Z.: Performance analysis of dynamic PCA for closed-loop process monitoring and its improvement by output oversampling scheme. IEEE Trans. Control Syst. Technol. **27**(1), 378–385 (2019)
6. Qin, Y., Yan, Y., Ji, H., et al.: Recursive correlative statistical analysis method with sliding windows for incipient fault detection. IEEE Trans. Ind. Electron. **69**, 4185–4194 (2021)
7. Wang, G., Yin, S.: Enhanced quality-related fault detection approach based on OSC and M-PLS. IEEE Trans. Ind. Inf. 1 (2015)
8. Li, G., Qin, S.J., Zhou, D.: Geometric properties of partial least squares for process monitoring. Automatica **46**(1), 204–210 (2010)
9. Zhou, D., Li, G., Qin, S.J.: Total projection to latent structures for process monitoring. AIChE J. NA-NA (2009)
10. Yin, S., Ding, S.X.: Study on modifications of PLS approach for process monitoring. IFAC Proc. **44**, 12389–12394 (2011)
11. Peng, K., Zhang, K., Li, G.: Quality-related process monitoring based on total kernel PLS model and its industrial application. Math. Probl. Eng. **2013**, 1–14 (2013)
12. Zhang, Y., Sun, R., Fan, Y.: Fault diagnosis of nonlinear process based on KCPLS reconstruction. Chemom. Intell. Lab. Syst. **140**, 49–60 (2015)
13. Said, M., Abdellafou, K.B., Taouali, O.: Machine learning technique for data-driven fault detection of nonlinear processes. J. Intell. Manuf. **31**(4), 865–884 (2019)
14. Li, J., Yan, X.: Process monitoring using principal component analysis and stacked autoencoder for linear and nonlinear coexisting industrial processes. J. Taiwan Inst. Chem. Eng. **112**, 322–329 (2020)
15. Sun, C., Hou, J.: An improved principal component regression for quality-related process monitoring of industrial control systems. IEEE Access **5**, 21723–21730 (2017)

16. Jang, K., Hong, S., Kim, M., et al.: Adversarial autoencoder based feature learning for fault detection in industrial processes. IEEE Trans. Ind. Inf. **18**(2), 827–834 (2021)
17. Zamani, H., Bahrami, H.R., Garris, P.A., Mohseni, P.: Compressed principal component regression (C–PCR) algorithm and FPGA validation. IEEE Trans. Circ. Syst. II Express Briefs **67**(12), 3512–3516 (2020)
18. Lahdhiri, H., Taouali, O.: Reduced rank KPCA based on GLRT chart for sensor fault detection in nonlinear chemical process. Measurement **169**, 108342 (2021)
19. Xidonas, P., Tsionas, M., Zopounidis, C.: On mutual funds-of-ETFs asset allocation with rebalancing: sample covariance versus EWMA and GARCH. Ann. Oper. Res. **284**(1), 469–482 (2018). https://doi.org/10.1007/s10479-018-3056-z
20. Bakdi, A., Kouadri, A.: A new adaptive PCA based thresholding scheme for fault detection in complex systems. Chemom. Intell. Lab. Syst. **162**, 83–93 (2017)
21. Song, B., Shi, H.: Fault detection and classification using quality-supervised double-layer method. IEEE Trans. Ind. Electron. **65**(10), 8163–8172 (2018)
22. Adeli, M., Mazinan, A.H.: High efficiency fault-detection and fault-tolerant control approach in Tennessee Eastman process via fuzzy-based neural network representation. Complex Intell. Syst. **6**(1), 199–212 (2019). https://doi.org/10.1007/s40747-019-0094-3
23. Sun, Y., Qin, W., Zhuang, Z., Xu, H.: An adaptive fault detection and root-cause analysis scheme for complex industrial processes using moving window KPCA and information geometric causal inference. J. Intell. Manuf. **32**(7), 2007–2021 (2021). https://doi.org/10.1007/s10845-021-01752-9